Ceramics International 47 (2021) 4455–4465

Contents lists available at ScienceDirect

Ceramics International

journal homepage: www.elsevier.com/locate/ceramint

Femtosecond Ti: Sa ultra short-pulse laser irradiation effects on the properties and morphology of the zirconia surface after ageing

Vanessa Harumi Kiyan [a], Flávia Pires Rodrigues [a,b], Ricardo Elgul Samad [c], Denise Maria Zezell [c], Marco Antonio Bottino [d], Nelson Batista De Lima [e], Cintia Helena Coury Saraceni [a,*]

[a] Post-Graduate Programme in Dentistry, Paulista University - UNIP, Rua Dr. Bacelar 1212, 04026-002, Vila Clementino, São Paulo, SP, Brazil
[b] Post-Graduate Programme in Dentistry, Federal University of Ceará, Rua Monsenhor Furtado s/n, Rodolfo Teófilo, 60430-355, Fortaleza, CE, Brazil
[c] Centro de Lasers e Aplicações, IPEN/CNEN-SP, Av. Prof. Lineu Prestes 2242, 05508-000, Cidade Universitária, São Paulo, SP, Brazil
[d] Institute of Science and Technology of São José Dos Campos (ICT-UNESP), Av. Eng. Francisco José Longo, 777, 12245-000, Jd. São Dimas, São José Dos Campos, SP, Brazil
[e] Center for Material Science and Technology-Nuclear and Energy Research Institute, IPEN-SP, Av. Prof. Lineu Prestes 2242, 05508-000, Cidade Universitária, São Paulo, SP, Brazil

ARTICLE INFO

Keywords:
Y-TZP Zirconia
Ultrashort laser pulses ablation
Surface treatment
Bi-axial flexure strength

ABSTRACT

Femtosecond pulses from a Ti:Sapphire laser were used to irradiate specimens of yttria-stabilised (35% mol) tetragonal zirconia (Y-TZP) with the purpose of studying the effects of the irradiations on their surface properties and morphology after ageing. Zirconia disks were divided into eight groups (n = 32) according to their surface treatment and subsequent ageing: Control: no treatment; sandblasting: Al_2O_3 sandblasting 50 μm; and ultrashort laser pulses irradiation with 25 μJ pulses, considering two different scanning steps based on the width between two grooves. These groups were duplicated and submitted to ageing. The surfaces were analysed using scanning electron microscopy (SEM), and X-ray diffraction. A finite element analysis, a biaxial flexure test, as well as fractographic and Weibull analyses, were performed. The strengths of the disks were statistically different for the treatment factor, and the principal stresses seemed to be concentrated at the centre of the specimens, as predicted by the computer simulations. Ageing decreased the strengths for all groups and increased the Weibull modulus for the laser group with the 40 μm-width between two grooves. The sandblasting group presented the highest monoclinic phase peak. Although the most significant strength was found within the sandblasting group, the phase transformation was favourable to the laser groups. The Weibull modulus was higher for the laser group with the 60 μm-width between two grooves, confirming the highest homogeneity of its failure distribution. Regardless of the surface treatment, strength was decreased with ageing in all groups. The femtosecond Ti:Sa ultra-short pulse laser irradiation can be suggested as an alternative to the gold standard sandblasting in long-term Y-TZP zirconia rehabilitations, such as crowns and veneers.

1. Introduction

The zirconia-based ceramics are on the top of the evolution of new ceramic materials associated with advanced technologies [1], particularly for dental crowns and veneers. The morphology and mechanical properties of the zirconia used for these restorations have been then essential factors to be further considered.

Due to its well-known mechanical properties, biocompatibility, and chemical stability, the yttria-stabilised (35% mol) tetragonal zirconia (Y-TZP) is eligible for clinical applications [2–5], contributing to the longevity of the dental ceramic restorations. When the Y-TZP goes from the tetragonal to the monoclinic phase transformation (T → M), there is a 4.5 %-volume increase that creates a compression zone around an incipient crack that makes its propagation difficult and increases material strength [1,4,6–8]. However, despite the positive initial transformation effect on strength, when zirconia experiences excessive stress promoted by finishing, surface treatment, phase transformation, or even ageing, this phase transformation may be more pronounced. This increase in phase transformation can lead to an initial crack that may propagate throughout the material, detaching zirconia grains. Cracks or grain detachments may generate roughness and compromise strength and fracture toughness [4,8–10].

* Corresponding author. Rua Dr. Bacelar, 1212, 4° Andar, São Paulo, SP, 04026-002, Brazil.
E-mail address: cintiahcsaraceni@gmail.com (C.H. Coury Saraceni).

https://doi.org/10.1016/j.ceramint.2020.10.006
Received 9 July 2020; Received in revised form 9 September 2020; Accepted 2 October 2020
Available online 7 October 2020

The bonding phenomenon between the zirconia surface and the resin-based cement in ceramic rehabilitation is not yet fully understood and remains to be a challenge. As it is an acid-resistant ceramic, the adhesive cementation technique using a resin-based cement becomes critical. Different surface treatments have been proposed to overcome the challenge of ceramic-cement bonding, to avoid the cement retention decrease, fracture strength, and marginal adaptation [11–13]. Some treatment options have been reported to date, such as aluminium oxide sandblasting, silica oxide sandblasting, liner applications, acid etching, and various laser irradiations [8,14].

The use of 50 μm Al_2O_3 particles at moderate pressure (0.25 MPa) was recently recommended, with clinical evidence [15]. On the other hand, other studies mention that when using sandblasting onto zirconia, some alterations on the size of the particles, application time, and pressure may occur, which may lead to high stress [16,17]. Consequently, this surface treatment could lead to an excessive T→M phase transformation and flexural strength decrease [18,19], actively risking the longevity of future ceramic restorations [20]. For this reason, it is crucial to investigate what surface treatments would generate a more uniform surface morphology and better failure homogeneity distribution. These performances would positively promote no decrease in the zirconia stress when bonded to dentin with a resin-based cement, and consequently, reduce the probability of catastrophic failure rates.

Different laser irradiation methods and types have been considered as alternatives for zirconia surface treating, among which the CO_2, Nd:YAG, and the Er:YAG are the most used in Dentistry [12,16,21]. However, there are still no protocols which describe their parameters, ceramic surfaces [22,23]. Titanium:sapphire laser irradiation (also known as Ti:Sa lasers, Ti:Al_2O_3 lasers, or Ti:sapphs) has been pointed out as a promising alternative for zirconia surface treatment due to its precise ablation and generation of a sub micrometric heat-affected zone (HAZ) from the irradiation [24], with minimal structural changes or thermal damage due to its low-energy pulses [24,25].

For practical applications, the pulse energy must be amplified to the millijoule level, known as ultrashort pulse laser (USPL) [26,27,28]. Differently from the observed with the short (ns) and long pulse (μs) lasers, in which the thermomechanical ablation removes the tissue, the USPL ablation does not occur as a consequence of temperature increase, but from a plasma-mediated ablation [29–34].

Another negative aspect of the zirconia is its long-term degradation in a humid environment or with ageing, as previously reported in other studies, both in Dentistry and Medicine [35–37]. The humidity penetration exacerbates such process and extends the degradation to deeper layers, resulting in micro and macro crack propagations, reducing the flexural strength [5,35–37]. In this process, the T→M phase transformation occurs even with the addition of tetragonal phase stabilisers, as the induced stress of grain-adjacent areas caused by grain increase in volume might be high enough to generate microcracks propagation. According to Chevalier et al., 1 h of ageing in an autoclave at 134 °C, under 0.2 MPa would correspond to 3–4 years of an *in vivo* scenario [38].

Considering the limitations and implications that zirconia may present to restorations in terms of clinical longevity, this paper aims to evaluate the effects of the femtosecond Ti:Sa laser as a surface treatment for zirconia. To date, most studies have been considering the investigation of bonding with shear tests only, with no morphological, structural, or ageing approaches [3,11,12,21,33]. The biaxial flexure strength test was the one with the most clinically relevant scenario and the most reliable [39,40]. Moreover, there is no data of zirconia treated with Ti:Sa with ultra-short laser pulses submitted to biaxial flexure strength testing, which motivated this study, and these results are being presented for the first time, to our knowledge. Therefore, this study evaluates the mechanical properties, morphology, and phase transformation of zirconia, after autoclave ageing [35,36,41] to simulate both temperature and pressure changes.

2. Materials and methods

2.1. Zirconia surface preparation and morphological analysis

Disks with 1.3 mm ± 0.1 mm in thickness and 15 mm in diameter (n = 256) were obtained from zirconia-based ceramic cylinders (VITA In-Ceram YZ for inLab 20/19, VITA, Zahnfabrik, Bad-Sackingen, Germany). The disks were sectioned with a specific equipment that consisted of a bench micromotor and a diamond disk (designed for this purpose).

Before the surface treatments, all disks were finished under cooling with 600; 1200; 2000; and 2500-grit sandpaper sheets, until a thickness between 1.1 mm ± 0.2 mm was achieved, and measured with a digital calliper of 0.001 mm accuracy (Mitutoyo™, Tokyo, Japan). The disks were then ultrasonically cleaned with distilled water for 10 min [42]. To assure they were free of cracks or visible fractures, they were observed through an optical microscope, with 40x magnification. The disks were then sintered in a specific oven (Ceramill™ therm 3 - Amann Girrbach AG-Dental-Systeme, Germany), with a sintering cycle that followed the zirconia manufacturer's specifications (1,530 °C; 400 °C). The final specimens were 12 mm and 0.8 mm ± 0.2 mm in diameter and thickness, respectively, following other recent studies using the ball-on-ring biaxial flexure test set-up for bilayer specimens [4,43–46].

The ceramic disks were randomly divided into eight groups (n = 32) and were submitted to three different surface treatments, analysed using X-ray diffraction (XRD), scanning electron microscopy (SEM), and submitted to a ball-on-ring biaxial flexure test, before and after ageing. The materials used in this study (information from the manufacturers) are presented in Table 1.

For the sandblasting group (*SB*), the zirconia surfaces were cleaned, dried, and sandblasted with Al_2O_3-50 μm, with 551.58 kPa (80 psi) of pressure for 10 s, 10 mm work distance. The particles contacted the zirconia perpendicularly [47–49]. The specimens from L and L-aged groups were irradiated to generate a series of grooves, with ultra-short laser pulses generated by a Ti:Sa amplified laser system with no manual contact (Femtopower Compact Pro CE-Phase HP/HR, Femtolasers, Austria). This system generates 25-fs (fs) pulses, centred at 785 nm with a bandwidth of 40 nm (FWHM), at a 4-kHz repetition rate in a beam with M2<2. For the irradiations, all performed at room temperature and with no sample cooling, the pulse energy was fixed at 25 μJ by changing the amplifier pockels cell voltage.

The specimens were mounted on a three-axis translation system (3 UTS100C translators integrated with a computer-controlled ESP301 driver, Newport, USA), and the laser beam was focused by a 75-mm focal length achromatic doublet (AC254-075-B, Thorlabs, USA) to a 20 μm, waist positioned on the sample surface with a perpendicular incidence. This unique system defined a 1.99 J/cm^2 fluence (energy density) per pulse, and the sample was moved to have its surface area irradiated by the laser beam in parallel lines, separated by a distance (Δy). The beam's travel speed was 8 mm/s, in parallel lines, as shown in Fig. 1. Two Δy displacements were used, based on the widths between every two grooves: 40 μm (group L_1) and 60 μm (group L_2), with micro groove depth varying within 4.3 ± 0.7 μm and 5.4 ± 1.1 μm, respectively. For each specimen, the interval between two groves was approximately 20 μm and remained identical in the horizontal direction during the experiment. The laser surface treatment parameters were determined in pilot tests.

After the surface treatment, all specimens were analysed using light microscopy before the scanning Electron Microscopy (SEM) (JEOL-JSM-6510, USA) to identify the presence of debris or any macro defect that could affect the SEM analysis. At this stage, the specimens were only zirconia monolayer disks. For the SEM morphological analysis after treatment, each sample was sputter-coated with a 15-nm thick palladium gold layer (SputterCoater MED-020-Bal-Tec).

Table 1
Materials used in this study (information from the manufacturers).

Material	Commercial presentation and manufacturer	Composition	Batch number #
Y-TZP Zirconia	VITA In-Ceram YZTM for in Lab 20/19, VITA, Zahnfabrik, Bad-Sackingen, Germany	ZrO_2 3% Y2O3, contaminants	24811
Resin Cement	Panavia F 2.0™, Kuraray Co. Ltd., Tokyo, Japan	Paste A: methacrylate, MDP, quartz glass, microfiller, photoinitiator Paste B: methacrylate, barium glass, sodium fluoride, chemical initiator.	000058
Silane	Clearfil Ceramic Primer Kuraray Co. Ltd., Tokyo, Japan	3-MPS, 10-MDP, ethanol	9C0014
Resin-composite	Filtek Z350 XT™, shade A2D 3 M ESPE, St. Paul, MN, EUA.	Bis-GMA, UDMA, TEGDMA, Bis-EMA, silica, zirconia	869894
Al_2O_3	Polidental Ind. & Com. Ltda, São Paulo, Brazil	Al_2O_3.50 μm	–

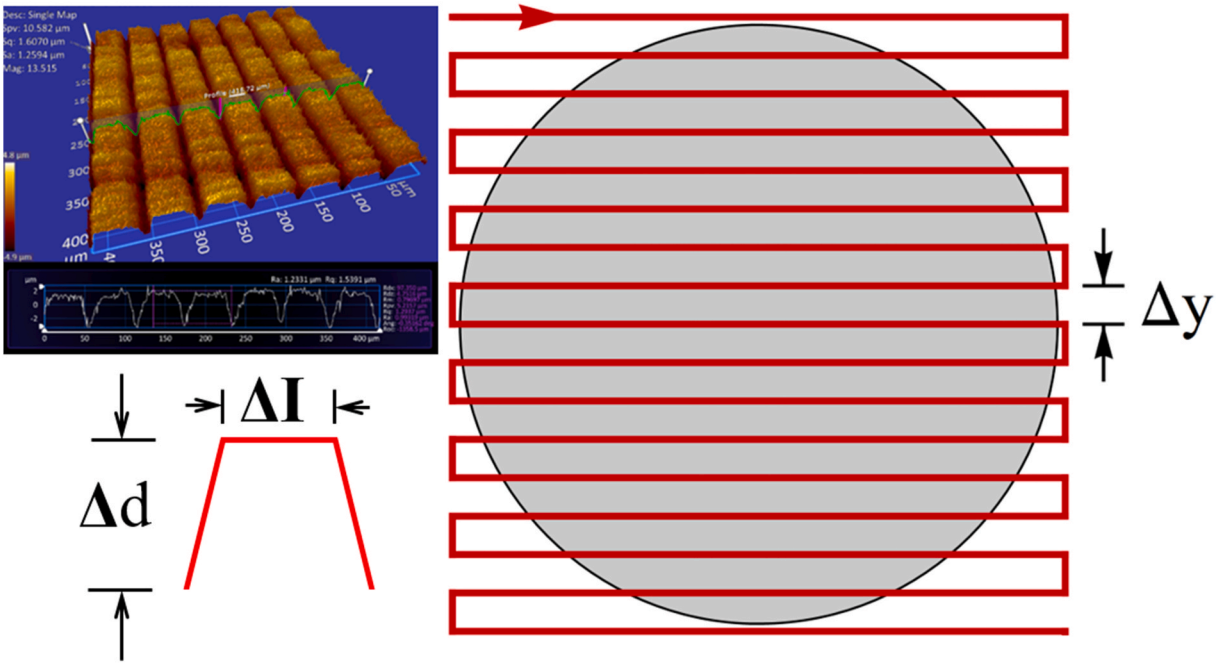

Fig. 1. Representation of the laser path used for each zirconia disk during a laser scanning.

2.2. X-ray diffraction analysis of the phase transformation

A quantitative analysis of phase transformation was carried out with an X-ray diffractometer (Multiflex, Rigaku, Tokyo, Japan). The Cu-Ka monochromatic radiation was set with the following parameters: 40 kV, 20 mA, with angular range varying from 25° to 90°, with 0.02° step, 3 s per step. The X-ray diffraction analysis was calculated with the application of the Rietveld Refined Method. This method was found to be better than the conventional Garvie-Nicholson equation, modified by Toraya, allowing the quantification of the monoclinic phase. This quantification is made by differentiating the peaks of tetragonal and cubic phases, using all the diffractogram peaks for calculation [3,50]. The phase was identified using the Crystallographica Search-Match™ software (Oxford Cryosystems, Oxford, UK), where the data obtained was compared to the ones available in the ICSD (Inorganic Crystal Structure Database) database. The Rietveld Refinement Method was used to calculate the percentages of the different phases using the GSAS software (GSAS; Larson and Von Dreele, USA, freeware).

2.3. Bilayered sample preparation

After treatment, all specimens were cleaned using ultrasound with distilled water for 10 min for residue removal before cementation [49].

Two hundred and forty specimens were cemented with the support of a polished resin-composite underneath the disk using Panavia F 2.0TM dual resin-cement (Kuraray Co. Ltd., Tokyo, Japan), manipulated according to the manufacturer's specifications. All treated surfaces were coated with Clearfil Ceramic Primer™ (Kuraray Co. Ltd., Tokyo, Japan), followed by a gentle air jet for excess removal. Equal parts of pastes A and B were dispensed, mixed for 20 s, and the cement was applied to the ceramic disk centres. Then, the assemblage was positioned on a glass-cover plate on top of the resin-composite (Filtek Z350 XT; flexural modulus = 11.4 GPa - 3 M ESPE, St. Paul, MN, USA, colour A2D) with 14-mm diameter and 2-mm thickness to simulate the dentine [43] (Fig. 2).

A 5N-load was applied to the cement for 60 s and then photo-polymerised for 60 s, with a LED light curing device (Bluephase G2 - Ivoclar, Vivadent), with 1500 mW/mm^2 [19,43]. The excess cement was carefully removed with a #15 scalpel blade. The cement-zirconia final thickness was measured, and the specimens out of the 100-150-μm range were discarded. The specimens were then stored in distilled water (Model: 3173253- Quimis- Brazil) at 37 °C for 24 h [43]. After this period, the specimens were submitted to a ball-on-ring biaxial flexure strength test.

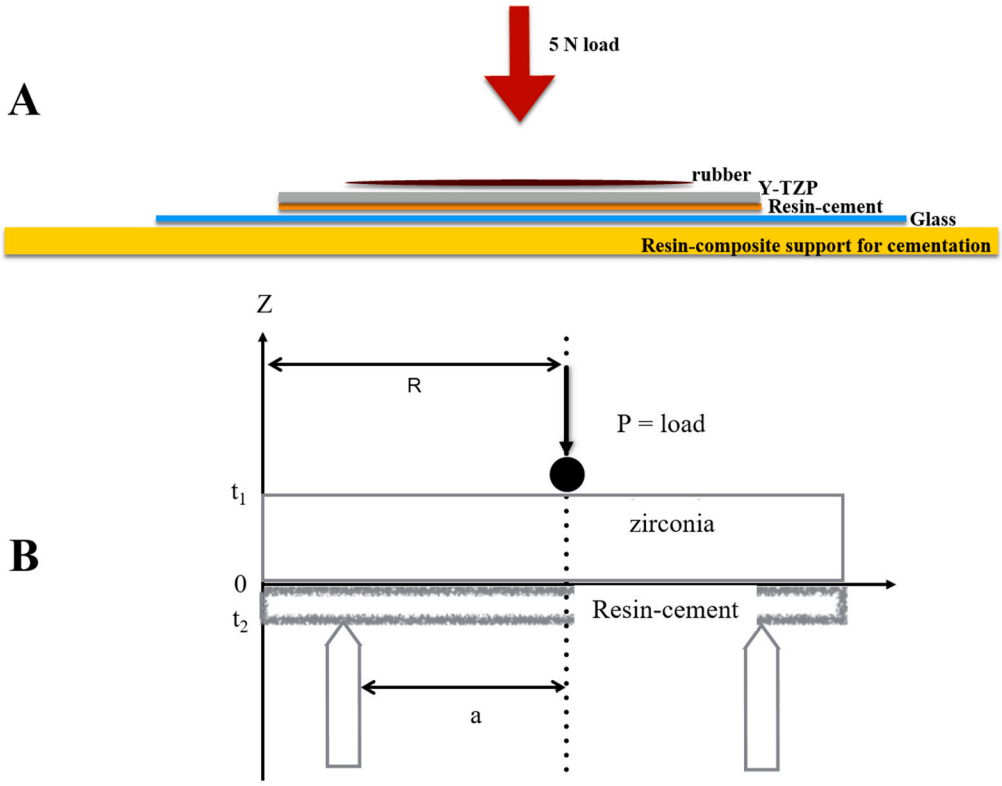

Fig. 2. Cementation representation (A) and the ball-on-ring biaxial flexure strength test set-up for a bilayer disk sample (adapted from Addison et al., 2010) [31].

2.4. Ageing

After following the preparation previously described for the BoR specimens on item 2.3, half of the specimens were aged for further mechanical testing in open autoclave-suitable tubes.

The ageing was performed in an autoclave (Dabi Atlante M9 Ultra Clave - Alliage S/A Indústrias Médico Odontológicas SP- Brazil) at 1340 °C and 2 Kgf/cm^2, for 20 h, following ISO 13,356 from 2008 [41, 50].

2.5. Finite element analysis

Three-dimensional models of finite elements were obtained according to the geometry of the specimen used in the experimental test performed in item 2.5, and pre and post-processed in the MSC.PATRAN program (version 2017, MSC. Software, USA). The models were linearly analysed in the MSC. Marc program (version 2013, MSC. Software, USA) before being post-processed again for the interpretation of the results in MSC.PATRAN.

The models consisted of three-dimensional, 8-node hexahedral elements (Hex8), obtained by the extrusion of 4-node quadrilateral elements (Quad4). The finished models presented an average of 13,440 nodes (vertices of hexahedral elements) and 11,886 elements. The interface nodes were shared between the two materials, representing perfect adhesion [51].

In MSC. PATRAN, the boundary conditions applied to the models were the following:

- Displacement: in all models, the symmetry-face nodes were fixed. To represent the ring in which the specimens were placed before testing (10 mm in diameter), the nodes of a radial line corresponding to the radius of 5 mm were fixed in the vertical direction only. The nodes were free for lateral displacement.
- Load: for each model, a 100-N load was applied at the piston corresponded area (4-mm diameter - in this case, 2-mm radius, following the represented symmetry).
- Materials: all materials were considered linear, elastic, homogeneous, and isotropic. The elastic modulus and Poisson's ratio for the zirconia and the resin-cement were 209.3GPa/0.25 and 18.3 GPa/0.27, respectively, according to the manufacturer. The maximum principal stresses and the maximum principal deformations (tensile) were recorded for all cases and represented in colour fringes for comparison.

2.6. Biaxial flexure test – ball-on-ring (BoR)

The specimens were submitted to the ball-on-ring biaxial flexure test using a universal testing machine (Model: KE.2.000 MP - Kratos- Brazil). The loads after rupture (N) were recorded, and the stresses generated in the zirconia were calculated. All disks were tested in contact with a 0.2-mm thickness piece of latex between the sample and the load applicator tip. This piece was used to compensate any variations in geometry and to allow small lateral displacement, minimising shear friction, as well as any contact-induced damage [20].

The disks were carefully positioned and aligned on the ring-shaped support. The load was applied with an indenter of 4 mm in diameter to the centre at 0.5 mm/min. The central thickness of each fractured portion was measured to calculate the mean for each disk. The parameters considered for the analytical calculation were based on the study by Hsueh et al. [52]. Two-way ANOVA, the Dunnett's test, and the Tukey test ($\alpha = 0.05$) were applied using SPSS 21 program (Chicago, USA). The fracture resistance data was submitted to Weibull's analysis to determine the survival probability distributions. The confidence intervals (95%) were calculated, and the statistical difference was applied so that these intervals would be overlapped [53].

2.7. Fractographic analysis

Bilayer biaxial flexure fractured specimens were analysed with SEM (JEOL-JSM-6510, USA) to assess the possible failure features and fracture origin. Each sample was sputter-coated with a 15-nm thick palladium gold layer (SputterCoater MED-020-Bal-Tec).

3. Results and discussion

This study analyses some alternatives to the zirconia surface treatment for the extinguishing or decrease of a possible unpleasant phase transformation and fracture probability. For this purpose, two Ti:Sa ultra-short laser pulse irradiation conditions were considered: surface scanning by 40 and 60 μm separated lines (L_1 and L_2-groups). The mechanical properties and the morphology of the control (C), sandblasted (SB) and irradiated Y-TZP zirconia were analysed before and after ageing.

3.1. Zirconia surface preparation and morphological analysis

Initially, from the morphological analyses using SEM, the *C*-group specimens presented typical and expected manual finishing traces and some polishing grooves on their surfaces (Figs. 3-1A). On the other hand, after sandblasting (*SB*-group), despite the zirconia's prominent but uniform groove presence (Fig. 3 – 2A and 2B), this *SB*-group revealed areas with more considerable surface damage with chipping and grooves than the control group. These grooves can be seen in higher magnification (1500x in Figs. 3–1B and 2B). A rough surface would be a positive factor, as it increases the surface energy and, consequently, its wettability if the cement surface tension and its viscosity are favourable. Additionally, for the other two groups, to which the femtosecond laser was applied, it was observed that this laser promoted surfaces of extended and homogeneous depressions (Fig. 3–B and 4B), similar to the one described by Kara et al. [11], which may better explain the failure distribution.

After the laser application, for both cases, the surface showed long uniform depressions, which correspond to the pulse's path, as the distance between the lows is regular and fit to the lateral displacement Δy (Fig. 1), between two laser lines, which may be verified in higher resolutions in Fig. 3–3A for 40 μm; and in Figs. 3–4A for 60 μm, respectively. These uniform depressions favour cement penetration, increasing the mechanical interlocking, as shown at the SEM images See Figs. 3-3B and 4B.

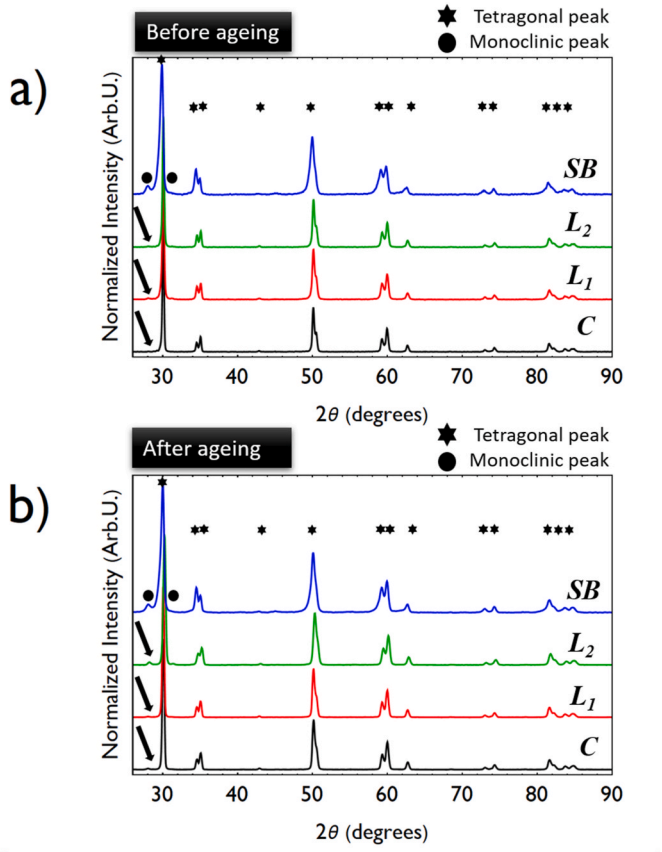

Fig. 4. X-Ray diffraction patterns for the experimental groups, before and after ageing.

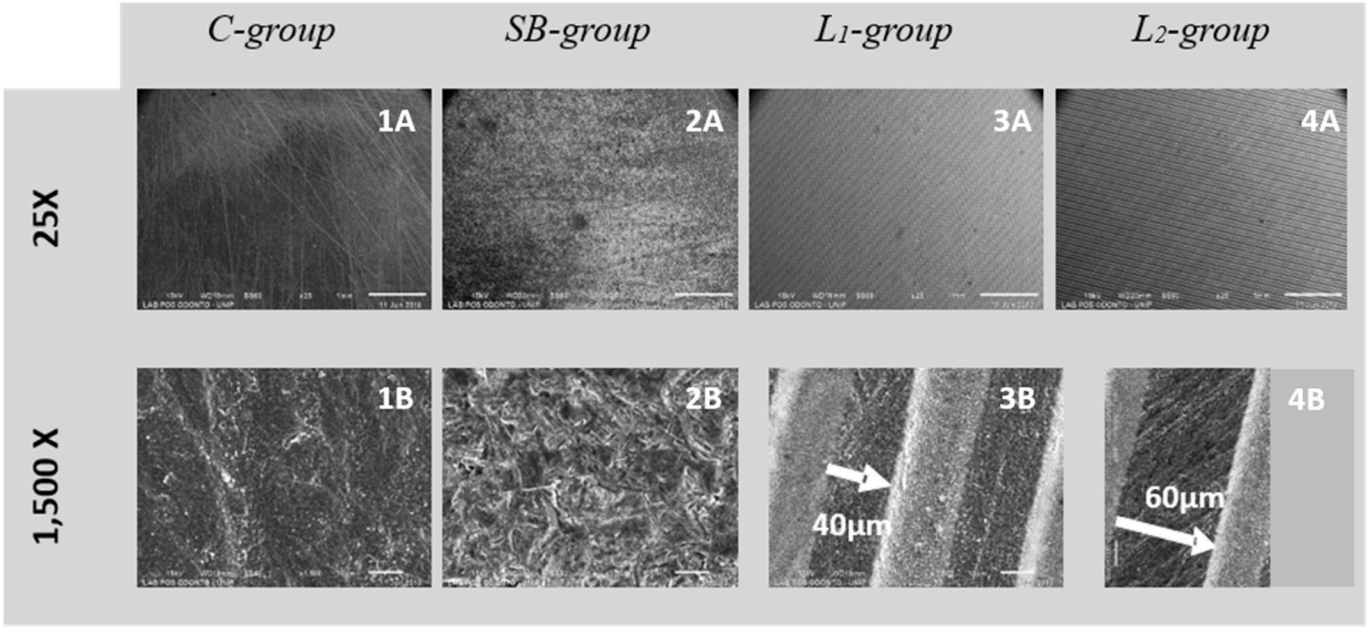

Fig. 3. SEM representative images of the Y-TZP surfaces after treatment.

3.2. X-ray phase transformation diffraction analysis

The X-ray diffraction graphs for all groups before and after ageing are presented in Fig. 4. The analysis provided percentages of crystalline phases for each group, calculated according to the Rietveld Refinement Method, are shown in Table 2. This method aims to obtain more advanced graphics, considering peaks that would be superposed (representing cubic and tetragonal phases). The application of this method allowed the cubic phase identification, and others possibly presented [55].

The phase transformation results from the X-ray diffraction revealed the high and dominant diffraction peaks for the tetragonal phase in all groups, as expected. A higher amount of cubic phase was verified in the *SB*-group, regardless of the ageing process. The presence of the cubic phase is not desirable as, according to some authors [10,54,55], it is formed by an yttrium-rich grain nucleation that leads to the decrease of this element in the tetragonal phase and, consequently, to ceramic instability in this phase.

Some authors [9,56,57] reported an increase in the monoclinic phase after sandblasting, which demonstrates the impact caused by this type of operator and technique-dependent treatment. In the present study, all other groups presented phase alterations after ageing, in amount, for each type. The amount of monoclinic phase was the highest for the *SB*-group (5%); however, it remained stable before and after ageing within the same group. L_2-group followed *SB* with the highest rate (5%) after ageing. The lowest phase alteration after ageing was found within the control group (1.5%). The higher amount of monoclinic phase could explain the reason this group presented the best absolute strength values and statistically significant higher characteristic strength, as a T→M phase transformation within the acceptable limits (25%) would generate a strength increase [54]. Accurately, for the monoclinic phase, both laser-irradiated groups showed antagonistic results: as this phase decreased for L_1, it increased up to the same amount of the *SB* group for L_2.

3.3. Ageing

The aged specimens' evaluation is fundamental as it represents the zirconia restorations' longevity in oral condition, in which degradation occurs due to the low temperature and humidity (LTD – low-temperature degradation) [49,58]. Although ageing is a well-known phenomenon, firstly described more than 30 years ago by Kobayashi et al. [59], little is known regarding its occurrence process.

The presence of the monoclinic phase was proven to be desirable right after sintering. However, it has been related to post-ageing surface damage, as degradation can occur. The ageing process promoted the monoclinic phase increase for the *C* and L_2 groups, and a decrease for *SB* and L_1. Some authors [60] demonstrated that there is no increase in the monoclinic phase after the ultrashort pulse laser irradiation in non-aged specimens. With ageing, however, this phase increased from 2 to 5% for L_2. The monoclinic phase increase would probably affect restoration stability, creating cracks on the zirconia surface, leading to its surface degradation [36], and it probably occurred during the low-temperature degradation in the wet state. Although the energy and pulse parameters were different from those applied in the other study, both laser groups still presented monoclinic phase increase lower than the 25%, as accepted by ISO 13356/2008 [61].

Table 2
Percentages of crystalline phases for the groups before and after ageing, calculated by the *Rietveld* method.

Phases	GROUPS							
	C	C-aged	SB	SB-aged	L_1	L_1-aged	L_2	L_2-aged
Monoclinic	_	1.5	5.0	5.0	2.0	1.4	2.0	5.0
Tetragonal	86.0	86.0	67.0	69.0	77.0	86.8	81.0	84.0
Cubic	14.0	12.0	28.0	25.0	21.0	11.7	17.0	10.0

3.4. Finite element analysis

The zirconia's maximum principal stress (MPa) and the maximum principal strain (mm/mm) are represented in Fig. 5. For both cases, the absolute values are not relevant, but their magnitude, represented here by the colour fringes.

It was possible to verify that the region with the greater tensile stress at the interface is the centre of the specimen, as it presented greater displacement during the tensile test, experimentally, towards the Z-direction. The colour fringe images show the area with the higher maximum principal strains was the centre-base of the specimen, which also presented the most elevated stress in magnitude. The results of the stress and strain distributions from the finite element analysis reflect the probable fracture origin for the biaxial flexure specimens. The same stress patterns were found in other bilayers simulation studies [51,62]. If the BoR sample's fracture in the same way, it means that the fracture probably occurred due to the inherent strength of the tested material and not due to non-uniform failure distribution, inclusions, or other process-related defects. This statement also reinforces the need for the Weibull analysis and the fractography as complementary steps to investigate each sample's behaviour.

To date, most studies have been evaluating the bond strength with shear tests only, with no morphological, structural or ageing approaches [3,11,12,16,33]. The biaxial flexure strength test was the one with the most clinically relevant scenario and the most reliable [63–66]. Moreover, there is no data referring to zirconia treated with Ti:Sa with ultra-short laser pulses submitted to a biaxial flexural strength test, which motivated this study.

3.5. Biaxial flexure test – ball-on-ring (BoR) and Weibull Analysis

Biaxial flexure strength (BFS) means and standard deviations (MPa), Weibull modulus (m), and the Y-TZP zirconia characteristic strength (σ_0), with different surface treatments, were used to replicate the finite element analysis failure pattern, followed by fractography. BoR results are presented in Table 3 and Fig. 6. There was no statistical difference among the groups neither before nor after ageing. After ageing, the control group did not generate specimens, as the cement detached from all zirconia specimens during the ageing process.

No statistical differences were found for the biaxial flexure strength in the present study, regardless of the ageing processing. Some authors have already pointed out the aluminium oxide sandblasting as 'gold standard' zirconia surface treatment in clinical practice [10,15,17,47], even with different particle sizes, application time, and pressure [57,67]. Zhang et al. [20] reported that although the Al_2O_3 sandblasting has been regarded as 'gold standard', they cause severe effects onto the zirconia as deep as 4 μm from the surface.

Some studies stated that although the surface treatments promoted bond strength increase between the zirconia and the cement (and the veneer) [68], they may lead to changes in the zirconia mechanical properties [15,39]. Some authors found a decrease in biaxial flexure strength after sandblasting, justified by the particle size and application time, which led to an excessive tetragonal-to-monoclinic phase transformation (T → M) [18,19,47]. Moreover, it has also been mentioned that although this abrasion can improve the roughness of the zirconia surface, a minimal undercut can be formed, and the abrasion does not lead to sufficient surface toughness as a result of high surface hardness. In the present study, the sandblasting proved to suffice for an immediate but inconsistent long-term bonding performance, considering the low Weibull modulus. Thus, other aspects must be verified as to ensure the clinical success and longevity of zirconia restorations.

External factors, such as mechanical stress caused by machining or by finishing and polishing processes with the zirconia, and the

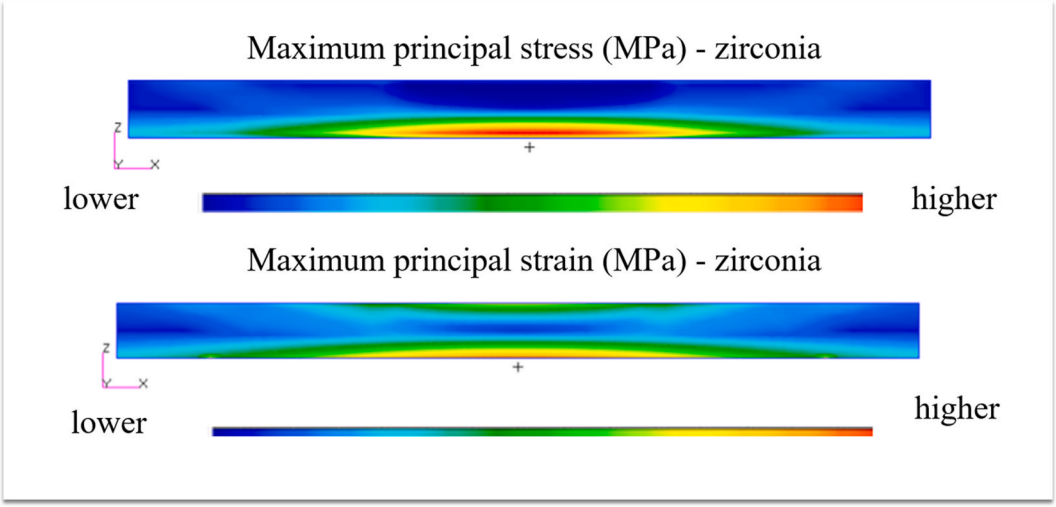

Fig. 5. Maximum principal stress (MPa) and maximum principal strain (mm/mm) at the zirconia, representatives of the biaxial flexure strength test.

Table 3
Biaxial flexure strength means (**BFS**) and standard deviations (MPa); Weibull modulus (***m***), and the characteristic strength (σ_0) of the Y-TZP zirconia with different surface treatments.

Groups	BS (MPa)	m	95% confidence interval of *m*	σ_0	95% confidence interval of the σ_0
C	1,137.8 (154.6) ^{A}	8.9 ^{b}	8.0–9.9	1,201.8 ^{b}	1,138.5–1,265.1
C-aged	–	–	–	–	–
SB	1,343.2 (224.7) ^{Aa}	7.1 ^{b}	6.7–7.5	1,434.3 ^{a}	1,382.7–1,485.9
SB-aged	1,199.8 (225.2)^{Aa}	5.9 ^{c}	5.4–6.3	1,296.2 ^{b}	1,254.1–1,338.4
L_1	1,115.0 (190.2) ^{Aa}	7.0 ^{b}	6.4–7.6	1,191.8 ^{b}	1,142.2–1,243.4
L_1-*aged*	1,034.8 (96.1) ^{Aa}	12.7 ^{a}	12.0–13.5	1,077.1 ^{b}	988.2–1,165.9
L_2	1,038.0 (166.6) ^{Aa}	7.4 ^{b}	6.8–8.1	1,106.0 ^{b}	1,053.8–1,157.6
L_2-*aged*	976.7 (143.0) ^{Aa}	8.2 ^{b}	7.5–8.9	1,035.7 ^{b}	978.9–1,092.6

Different letters mean a statistical difference in each column only. There is no comparison between lines.
In the first column, capital letters compared the groups before ageing and lowercase letters compared the aged groups.
(by ANOVA and Tukey; $p = 0.0001$; $\alpha = 0.05$).

degradation in the water environment (including the number of cycles), may also lead to phase transformation and a possible decrease in the zirconia flexural strength [49].

The ageing process seemed to not affect the biaxial flexural strength in the present study, as no statistical difference was detected before and after ageing. However, a decrease in the absolute strengths, and supported by Pereira et al. [58], showed that ageing decreases the biaxial flexure strength, fact that is also endorsed by Inokoshi et al. [69]. The ageing protocol used in this study was possibly not enough to affect the zirconia structure to the same extent as in those studies. However, the biaxial flexure strength shall not be evaluated without failure distribution data analysis. This analysis was the reason the Weibull analysis was performed, in which the Weibull modulus (m) was a valuable criterion to determine the quality of specimens. This analysis has been described as ideal for verifying the homogeneity of the biaxial flexure strength, as it reflects the result of the failure type on the sample structure.

From the Weibull Analysis findings, the *SB* group showed significantly higher characteristic strength (1,434.3 MPa, $p < 0.0001$). All other groups with lower characteristic strength presented no statistical difference among each other. The highest Weibull modulus was for the L_1-aged group ($m = 12.7$) and the lowest for the *SB*-aged group ($m = 5.9$) with statistical differences when compared to the other groups.

The Weibull modulus for dental ceramics ranges from 5 to 15 [70]. The present study results ranged from 5 to 13, with the highest statistically significant value for L_1-aged. The higher the Weibull modulus, the more homogeneous the failure distribution, and the lesser dispersive the mechanical test data, the higher the structural stability, which was confirmed by the lower standard deviation for the L_1-aged group on the biaxial flexural strength. This study has already demonstrated that by using the finite element analysis, the specimens would ideally be fractured in the centre of the disks. However, this method could only predict the probable origin of the fracture and not its direction of propagation, and neither how the possible defects would be guiding such propagation.

Considering the clinical reality, where restorations are aimed to be long-term rehabilitations, therefore aged, the laser surface treatment would be promising for the survival of these restorations, mainly following the L_1-aged protocol. Therefore, a treatment that promotes a higher modulus may be an indicator of a right clinical approach, even when the biaxial flexure strength is a little lower, considering this parameter represents more uniform and homogeneous failure distribution [70].

Considering the characteristic strength (or Weibull scale (σ_0)), the SB group presented higher results than the laser groups, which could reveal its lower failure probability. Sandblasting has been reported to either increase or decreases the flexural strength of zirconia, depending on the surface damage generated by the treatment, usually depending on the alumina particle size. As the surfaces were recorded before bonding and testing, it was easy to see that a uniformly rough surface was formed, probably resulting from the removal of some small and weakly attached grain, also eliminating the milling and grinding trace lines [19]. This uniformity can be related to the characteristic strength found for this group, however not for its modulus. The characteristic strength is a parameter that assumes a 63%-failure probability for the materials, defining how high or low the specimens rupture will be. It should ideally be high. However, *m* and σ_0 must be concomitantly analysed. When considered together, these parameters were favourable to L_1-aged, indicating that the failure probability due to the presence of a more substantial defect is lower than the one for *SB* and *C*. If L_1-aged is more homogeneous than *SB* and other groups, the defect probability is more moderate.

When comparing the laser groups, L_1-aged presented higher Weibull

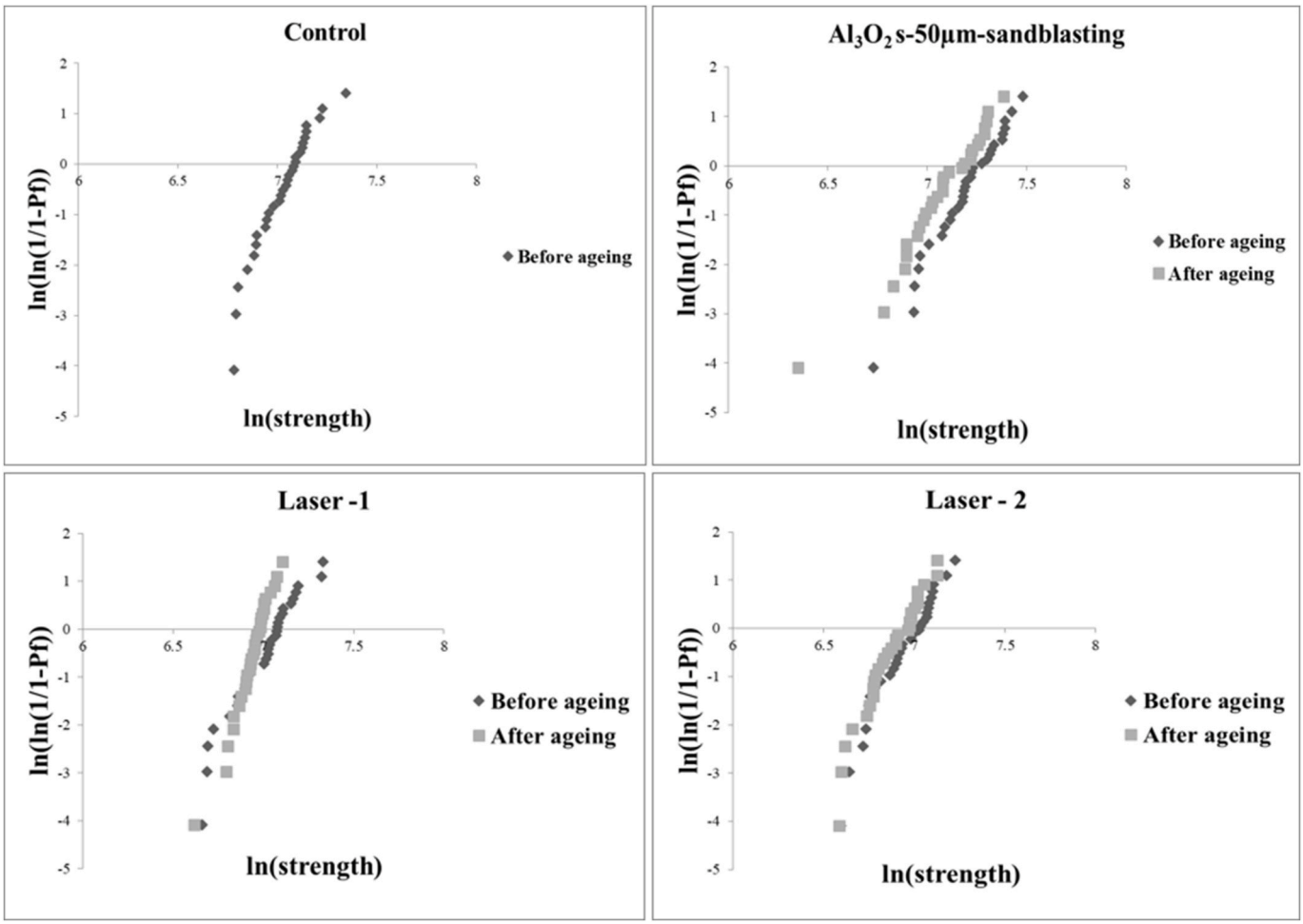

Fig. 6. *Weibull* plots for all groups.

modulus than L_2-aged. A possible explanation for the better failure distribution is the higher surface uniformity as a function of the smaller distance between the irradiation pulse scanning lines ($L_1 = 40$ µm and $L_2 = 60$ µm) and consequent greater irradiated area. Within the *C*-group, after the ageing process, all specimens had the cement detached from the zirconia surface. It is possible to affirm that the cement *per se* is not enough to ensure excellent clinical performance. The binomial cement-surface treatment is fundamental and indispensable to provide excellent clinical performance for the zirconia, and it was proven to be probably one of the reasons for the superior performance of the sandblasting surface treatment in the present study. The cement variation and investigation were not the focus of this study. However, the choice for the cement used in this research was based on previous studies, which indicated that functional MDP (10-methacryloxydecyl dihydrogen phosphate) monomer-based dental cement ester group were the most noted for the promotion of bonding with the metallic oxides present in the zirconia [48,69,71].

3.6. Fractographic analysis

SEM representative images from the fractographic analysis were selected to illustrate the failure distributions in each group (Fig. 7). For the control group, the images for the aged specimens were not obtained, as previously mentioned. The highlighted areas represent the possible fracture origin of the zirconia-cement interface.

The fractographic analysis showed discontinuities at the zirconia limit for the *C*-group. Fig. 7 – Control – A shows arrest lines with no defined mirror area. There was some discontinuity at the edge of the cement-zirconia interface. These discontinuities suggest multiple fractures caused by incomplete sintering or machining failures. Fig. 7-Control-B shows a smoother mirror area with an agglomerate of small porosities on the interface representing the possible fracture origin, surrounded by a 'mist' with 'hackles' in a radial direction. In this case, the mirror width and radius were quite similar.

For the *SB*-group, the SEM representative image allowed the identification of a feature that suggested a typical inclusion flaw or porosity agglomerate, or even the presence of another crystalline phase. In Fig. 7 – *SB* –A, the highlighted area represented the possible zirconia-cement interface fracture origin. Arrest and twist lines guided the crack propagation direction. For Fig. 7 – *SB* - B, a darker area at the zirconia compression zone was identified. The X-ray diffraction confirmed the presence of another phase.

For both laser groups, no significant defect that could be solely responsible for the fracture was noticed along the interface. Areas that could represent material inclusion, surrounded by porosities, were also identified. For these specimens, the cement was not removed before SEM analysis so that the visualisation of the cement wave formation, which represented the filled depressions, and the cement viscosity, would not be a physical obstacle in the laser groups' performance.

Fig. 7-L_1-A represents the data obtained for L_1. The highlighted areas represent the possible fracture origins at the zirconia-cement interface, and it is possible to see the arrest lines. In Fig. 7-L_1-B, a dark spot could mean material inclusion, surrounded by porosities. In Fig. 7-L_1-aged-A and B, after ageing, the cement penetration was enough to fill the depressions promoted by the laser pulses. The sample storage after the test generated gaps, which made the cement detached in some areas, as

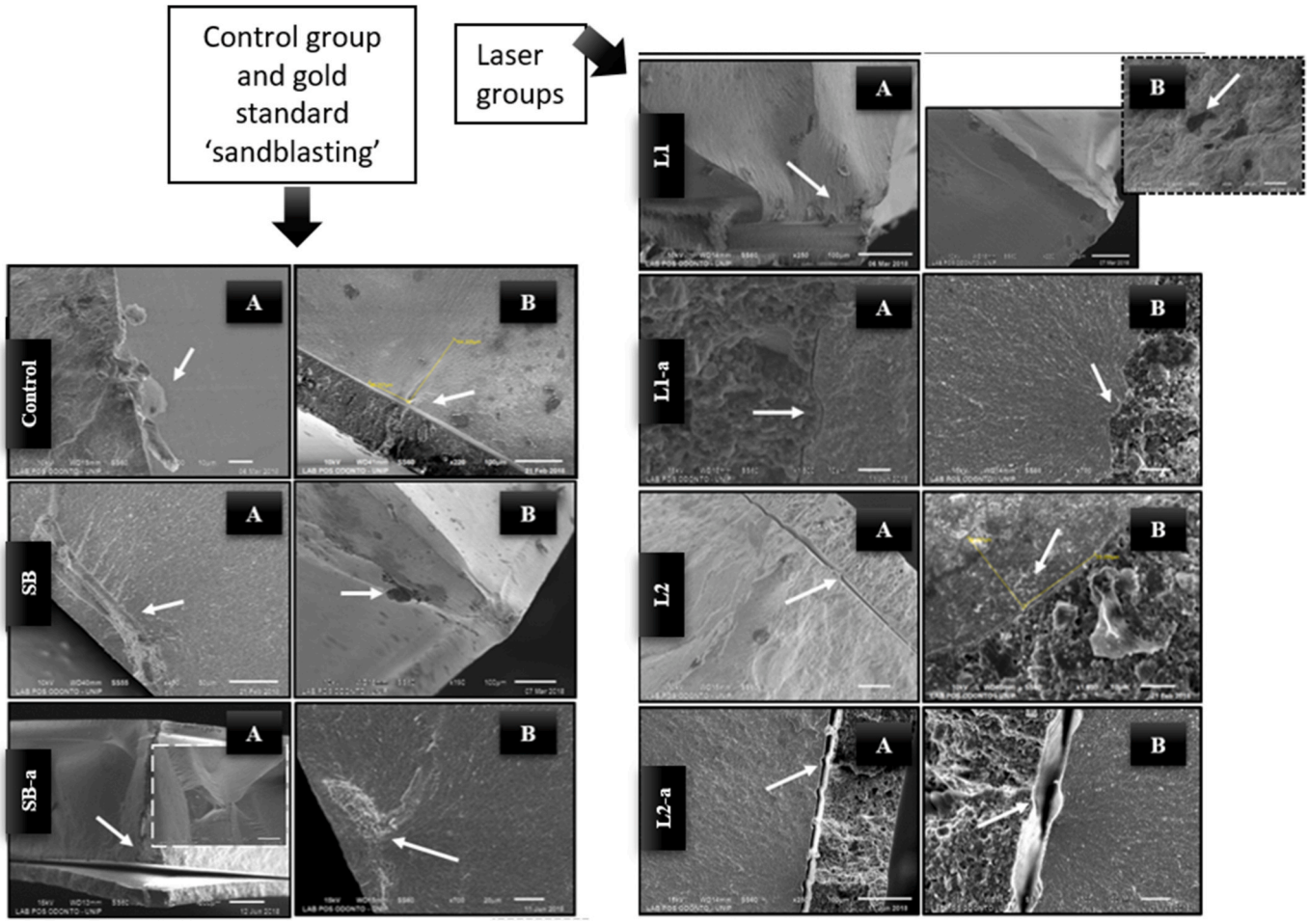

Fig. 7. SEM fractographic representative image for all groups: (A) and (B) are showing different features and/or the possible origin of the fracture.

mentioned above. For Fig. 7-L_1-aged-B sample, a region was formed to identify the mirror region created from an agglomerate of small porosities at the interface region.

In Fig. 7-L_2-A, an area with defined arrest lines was identified, guiding the direction of the crack propagation. For Fig. 7-L_2-B, a mirror with a similar width and radius was also found. For the aged specimens, Fig. 7-L_2-aged,images A and B presented and highlighted the possible fracture origin with a more defined mirror.It is possible to identify agglomerated porosities on the cement in both images.

The data obtained in this study must be interpreted with caution, considering a clinical scenario, as it is already well-known that the zirconia strength is, *per se*, high. However, the possibility of catastrophic failures added to the patient's variable diet and hygiene, and all the factors discussed here may also affect the zirconia performance *in vivo*. Thus, it might be possible to consider that the femtoseconds Ti:Sa ultrashort laser pulse irradiation is a promising zirconia surface treatment. Its homogeneity in failure distribution after ageing suggests a better long-term clinical performance. Future studies that evaluate other irradiation or ageing parameters should be carried out to define clinical protocols for the use of femtoseconds Ti:Sa ultra-short pulse laser irradiation in clinical practice. Guidelines for the optimum storage time of such bonded specimens, and longer storage times (ageing) are necessary for the interpretation of factors that affect the bond strength between treated-zirconia and different types of cement.

4. Conclusion

Considering the parameters for the zirconia surface treatment in this study, it may be concluded that:

- Zirconia may present long-term stability after irradiation, according to parameters given in this study. The Ti:Sa laser irradiation with the L_1 parameter, after ageing, decreased the T→M phase transformation with the Rietveld method;
- Both laser parameters promoted surfaces with extended and homogeneous depressions, which may better explain failure distribution;
- After the biaxial flexure tests, the laser groups presented the highest failure distributions homogeneities after ageing, which suggests that such treatments may be considered as promising and conservative options for zirconia surface treatment;
- The ageing process decreased the characteristic strength only for the *SB*-group and improved the failure distribution homogeneity with the laser irradiation treatment for the L_1-aged group.

Declaration of competing interest

The authors declare that they have no known competing financial interests or personal relationships that could have appeared to influence the work reported in this paper.

Acknowledgements

This research has not received any specific grant from funding agencies from the public, commercial, or non-profit sectors.

References

[1] G.K.R. Pereira, M. Amaral, R. Simoneti, G.C. Rocha, P.F. Cesar, L.F. Valandro, Effect of grinding with diamond-disc and -bur on the mechanical behavior of a Y-TZP ceramic, J Mech Behav Biomed Mater 37 (2014) 133–140.

[2] N. Matsumoto, M. Yoshinari, S. Takemoto, M. Hattori, E. Kawada, Y. Oda, Effect of intermediate ceramics and firing temperature on bond strength between tetragonal zirconia polycrystal and veneering ceramics, Dent. Mater. J. 32 (2013) 734–743.

[3] I. Çaglar, N. Yanlkoglu, The effect of sandblasting, Er:YAG laser, and heat treatment on the mechanical properties of different zirconia cores, Photomed Laser Surg 34 (2016) 17–26.

[4] L.F. Guilardi, G.K.R. Pereira, V.F. Wandscher, M.P. Rippe, L.F. Valandro, Mechanical behavior of yttria-stabilised tetragonal zirconia polycrystal: effects of different aging regimens, Braz. Oral Res. 31 (2017) 1–10.

[5] J.W. Kim, N.S. Covel, P.C. Guess, E.D. Rekow, Y. Zhang, Concerns of hydrothermal degradation in CAD/CAM Zirconia, J. Dent. Res. 89 (2010) 91–95.

[6] R. Andreiuolo, S.A. Gonçalves, K.R.H.C. Dias, A zircônia na Odontologia Restauradora, Rev. Bras. Odontol. 68 (2011) 49–53.

[7] B.D. Jakubowicz-Kohen, M.J. Sadoun, T. Douillard, A.K. Mainjot, Influence of firing time and framework thickness on veneered Y-TZP discs curvature, Dent. Mater. 30 (2014) 242–248.

[8] T. Sawada, C. Schille, J. Zöldföldi, E. Schweizer, J. Geis-Gerstorfer, S. Spintzyk, Influence of a surface conditioner to pre-sintered zirconia on the biaxial flexural strength and phase transformation, Dent. Mater. 34 (2018) 486–493.

[9] A. Grigore, S. Spallek, A. Petschelt, B. Butz, E. Spiecker, U. Lohbauer, Microstructure of veneered zirconia after surface treatments: a TEM study, Dent. Mater. 29 (2013) 1098–1107.

[10] H.A. Prasad, N. Pasha, M. Hilal, G.S. Amarnath, V. Kundapur, M. Anand, et al., To evaluate effect of airborne particle abrasion using different abrasives particles and compare two commercial available zirconia on flexural strength on heat treatment, Int. J. Biomed. Sci. 13 (2017) 93–112.

[11] O. Kara, H.B. Kara, E.S. Tobi, A.N. Ozturk, H.S. Kilic, Effect of various lasers on the bond strength of two zirconia ceramics, Photomed Laser Surg 33 (2015) 69–76.

[12] S. Kasraei, L. Rezaei-Soufi, E. Yarmohamadi, A. Shabani, Effect of CO2 and Nd:YAG lasers on shear bond strength of resin cement to zirconia ceramic, J. Dent. 12 (2015) 686–694.

[13] M. Vicente, A.L. Gomes, J. Montero, E. Rosel, V. Seoane, A. Albaladejo, Influence of cyclic loading on the adhesive effectiveness of resin-zirconia interface after femtosecond laser irradiation and conventional surface treatments, Laser Surg. Med. 48 (2016) 36–44.

[14] E. Papia, C. Larsson, M. Du Toit, P.V. Von Steyern, Bonding between oxide ceramics and adhesive cement systems: a systematic review, J. Biomed. Mater. Res. B Appl. Biomater. 102 (2014) 395–413.

[15] M. Kern, Bonding to oxide ceramics - laboratory testing versus clinical outcome, Dent. Mater. 31 (1) (2015) 8–14.

[16] S. Arami, M. Hasani Tabatabaei, F. Namdar, N. Safavi, N. Chiniforush, Shear bond strength of the repair composite resin to zirconia ceramic by different surface treatment, J. Laser Med. Sci. 5 (2014) 171–175.

[17] M. Ozcan, M. Bernasconi, Adhesion to zirconia used for dental restorations: a systematic review and meta-analysis, J. Adhesive Dent. 17 (2015) 7–26.

[18] H. Wang, M.N. Aboushelib, A.J. Feilzer, Strength influencing variables on CAD/CAM zirconia frameworks, Dent. Mater. 24 (2008) 633–638.

[19] G.J.K. Cheung, M.G. Botelho, Zirconia surface treatments for resin bonding, J. Adhesive Dent. 17 (2015) 551–558.

[20] Y. Zhang, B.R. Lawn, E.D. Rekow, V.P. Thompson, Effect of sandblasting on the long-term performance of dental ceramics, J. Biomed. Mater. Res. B Appl. Biomater. 71 (2004) 381–386.

[21] S. Arami, M.H. Tabatabae, S.F. Namdar, N. Chiniforush, Effects of different lasers and particle abrasion on surface characteristics of zirconia ceramics, J. Dent. 11 (2014) 233–241.

[22] Y.Z. Akpinar, A. Kepceoglu, T. Yavuz, M.A. Aslan, Z. Demirtag, H.S. Kılıc, et al., Effect of femtosecond laser beam angle on bond strength of zirconia-resin cement, Laser Med. Sci. 30 (2015) 2123–2128.

[23] S.M. Unal, R. Nigiz, Z.S. Polat, A. Usumez, Effect of ultrashort pulsed laser on bond strength of Y-TZP zirconia ceramic to tooth surfaces, Dent. Mater. J. 34 (2015) 351–357.

[24] R.E. Samad, L.M. Machado, N.D. Vieira, W.D. Rossi, Ultrashort laser pulses machining, in: I. Peshko (Ed.), Laser pulses - Theory, Technology, and Applications, InTech, 2012, pp. 143–174.

[25] S. Link, C. Burda, B. Nikoobakht, M.A. El-Sayed, Laser-induced shape changes of colloidal gold nanorods using femtosecond and nanosecond laser pulses, J. Phys. Chem. B 104 (2000) 6152–6163.

[26] T. Brabec, C. Spielmann, P.F. Curley, F. Krausz, Kerr lens mode locking, Opt. Lett. 17 (1992) 1292–1294.

[27] D. Strickland, G. Mourou, Compression of amplified chirped optical pulses, Optic Commun. 56 (1985) 219–221.

[28] P. Maine, D. Strickland, P. Bado, M. Pessot, G. Mourou, Generation of ultrahigh peak power pulses by chirped pulse amplification, IEEE J. Quant. Electron. 24 (1988) 398–403.

[29] S. Nolte, C. Momma, H. Jacobs, A. Tunnermann, B.N. Chichkov, B. Wellegehausen, H. Welling, Ablation of metals by ultrashort laser pulses, J. Opt. Soc. Am. B 14 (1997) 2716–2722.

[30] B.C. Stuart, M.D. Feit, A.M. Herman, A.M. Rubenchik, B.W. Shore, M.D. Perry, Optical ablation by high-power short-pulse lasers, J. Opt. Soc. Am. B 13 (1996) 459–468.

[31] A.P. Joglekar, H. Liu, G.J. Spooner, E. Meyhofer, G. Mourou, A.J. Hunt, A study of the deterministic character of optical damage by femtosecond laser pulses and applications to nanomachining, Appl. Phys. B Laser Optic. 77 (2003) 25–30.

[32] B.-M. Kim, M.D. Feit, A.M. Rubenchik, E.J. Joslin, P.M. Celliers, J. Eichler, et al., Influence of pulse duration on ultrashort laser pulse ablation of biological tissues, J. Biomed. Optic. 6 (2001) 332.

[33] M.V. Prieto, A.L.C. Gomes, J.M. Martín, A.A. Lorenzo, V.S. Mato, A.A. Martínez, The effect of femtosecond laser treatment on the effectiveness of resin-zirconia adhesive: an in vitro study, J. Laser Med. Sci. 7 (2016) 214–219.

[34] M.O. Santos, A. Latrive, P.A.A. Castro, W. Rossi, T.M.T. Zorn, R.E. Samad, A. Z. Freitas, D. Zezell, Multimodal evaluation of ultra-short laser pulses treatment for skin burn injuries 8 (2017) 443–450.

[35] H.-T. Kim, J.-S. Han, J.-H. Yang, J.-B. Lee, S.-H. Kim, The effect of low temperature aging on the mechanical property & phase stability of Y-TZP ceramics, J Adv Prosthodont 1 (3) (2009) 113–117.

[36] V. Lughi, V. Sergo, Low temperature degradation -aging- of zirconia: a critical review of the relevant aspects in dentistry, Dent. Mater. 26 (2010) 807–820.

[37] H.A. Vidotti, J.R. Pereira, E. Insaurralde, A.L.P.F. Almeida, A.L. Valle, Thermo and mechanical cycling and veneering method do not influence Y-TZP core/veneer interface bond strength, J. Dent. 41 (2013) 307–312.

[38] J. Chevalier, L. Gremillard, S. Deville, Low-temperature degradation of zirconia and implications for biomedical implants, Annu. Rev. Mater. Res. 37 (2007) 1–32.

[39] V. Bielen, M. Inokoshi, J. Munck, F. Zhang, K. Vanmeensel, S. Minakuchi, et al., Bonding effectiveness to differently sandblasted dental zirconia, J. Adhesive Dent. 17 (2015) 235–242.

[40] K. Lundberg, L. Wu, E. Papia, The effect of grinding and/or airborne-particle abrasion on the bond strength between zirconia and veneering porcelain: a systematic review, Acta Biomater Odontol Scand 3 (2017) 8–20.

[41] G.K.R. Pereira, A.B. Venturini, T. Silvestri, K.S. Dapieve, A.F. Montagner, F.Z. M. Soares, et al., Low-temperature degradation of Y-TZP ceramics: a systematic review and meta-analysis, J Mech Behav Biomed Mater 55 (2015) 151–163.

[42] H. Yamaguchi, S. Ino, N. Hamano, S. Okada, T. Teranaka, Examination of bond strength and mechanical properties of Y-TZP zirconia ceramics with different surface modifications, Dent. Mater. J. 31 (2012) 472–480.

[43] A.O. Spazzin, A. Bacchi, R. Alessandretti, M.B. Santos, G.R. Basso, J. Griggs, et al., Ceramic strengthening by tuning the elastic moduli of resin-based luting agents, Dent. Mater. 33 (2017) 358–366.

[44] O. Addison, A. Sodhi, G.J.P. Fleming, Seating load parameters impact on dental ceramic reinforcement conferred by cementation with resin-cements, Dent. Mater. 26 (2010) 915–921.

[45] A.K.F. Costa, A.L.S. Borges, G.J.P. Fleming, O. Addison, The strength of sintered and adhesively bonded zirconia/veneer-ceramic bilayers, J. Dent. 42 (2014) 1.

[46] T. Sawada, C. Schille, V. Wagner, S. Spintzyk, E. Schweizer, J. Geis-Gerstorfer, Biaxial flexural strength of bilayered disk composed of ceria-stabilised zirconia/alumina nanocomposite (Ce-TZP/A) and veneering porcelain, Dent. Mater. 34 (2018) 1199–1210.

[47] M. Saka, B. Yuzugullu, Bond strength of veneer ceramic and zirconia cores with different surface modifications after microwave sintering, J Adv Prosthodont 5 (2013) 485–493. 6.

[48] J.-J. Lee, J.-Y. Choi, J.-M. Seo, Influence of nano-structured alumina coating on shear bond strength between Y-TZP ceramic and various dual-cured resin cements, J Adv Prosthodont 9 (2017) 130–137.

[49] T. Cakir-Omur, R. Gozneli, Y. Ozkan, Effects of silica coating by physical vapor deposition and repeated firing on the low-temperature degradation and flexural strength of a zirconia ceramic, J. Prosthodont. 1–9 (2017).

[50] G.K.R. Pereira, C. Muller, V.F. Wandscher, M.P. Rippe, C.J. Kleverlaan, L. F. Valandro, Comparison of different low-temperature aging protocols: its effects on the mechanical behavior of Y-TZP ceramics, J Mech Behav Biomed Mater 60 (2016) 324–330.

[51] D. Zhang, J. Zhou, S. Zhang, L. Wang, S. Dong, Theoretical analyses and numerical simulations on the mechanical strength of multilayers subjected to ring-on-ring tests, Mater. Des. 51 (2013) 1–11.

[52] C.H. Hsueh, M.J. Lance, M.K. Ferber, Stress distributions in thin bilayer discs subjected to ball-on-ring tests, J. Am. Ceram. Soc. 88 (2005) 1687–1690.

[53] M. Amaral, L.F. Valandro, M.A. Bottino, R.O.A. Souza, Low-temperature degradation of a Y-TZP ceramic after surface treatments, J. Biomed. Mater. Res. B Appl. Biomater. 101 (2013) 1387–1392.

[54] J. Chevalier, S. Deville, E. Münch, R. Jullian, F. Lair, Critical effect of cubic phase on aging in 3 mol% yttria-stabilised zirconia ceramics for hip replacement prosthesis, Biomaterials 25 (2004) 5539–5545.

[55] A. Arata, T.M.B. Campos, J.P.B. Machado, D.R.R. Lazar, V. Ussui, N.B. Lima, et al., Quantitative phase analysis from X-ray diffraction in Y-TZP dental ceramics: a critical evaluation, J. Dent. 42 (2014) 1487–1494.

[56] D. Liu, J.P. Matinlinna, J.K.H. Tsoi, E.H.N. Pow, T. Miyazaki, Y. Shibata, et al., A new modified laser pretreatment for porcelain zirconia bonding, Dent. Mater. 29 (2013) 559–565.

[57] J.Y. Song, S.W. Park, K. Lee, K.D. Yun, H.P. Lim, Fracture strength and microstructure of Y-TZP zirconia after different surface treatments, J. Prosthet. Dent 110 (2013) 274–280.

[58] G.K.R. Pereira, M. Amaral, P.F. Cesar, M.C. Bottino, C.J. Kleverlaan, L.F. Valandro, Effect of low-temperature aging on the mechanical behavior of ground Y-TZP, J Mech Behav Biomed Mater 45 (2015) 183–192.

[59] K. Kobayashi, H. Kuwajima, T. Masaki, Phase change and mechanical properties of ZrO2-Y2O3 solid electrolyte after ageing, Solid State Ionics 3–4 (1981) 489–493.

[60] M. Aivazi, F.M. Hossein, F. Nejatidanesh, V. Mortazavi, B. HashemiBeni, J. P. Matinlinna, et al., The evaluation of prepared microgroove pattern by

femtosecond laser on alumina-zirconia nano-composite for endosseous dental implant application, Laser Med. Sci. 31 (2016) 1837–1843.
[61] M. Sehgal, A. Bhargava, S. Gupta, P. Gupta, Shear bond strengths between three different yttria-stabilised zirconia dental materials and veneering ceramic and their susceptibility to autoclave induced low-temperature degradation, Int J Biomater 2016 (2016).
[62] G.J.P. Fleming, P. Hooi, O. Addison, The influence of resin flexural modulus on the magnitude of ceramic strengthening, Dent. Mater. 28 (2012) 769–776.
[63] V. Bielen, M. Inokoshi, J. Munck, F. Zhang, K. Vanmeensel, S. Minakuchi, et al., Bonding effectiveness to differently sandblasted dental zirconia, J. Adhesive Dent. 17 (2015) 235–242.
[64] Y. Xu, J. Han, H. Lin, L. An, Comparative study of flexural strength test methods on CAD/CAM Y-TZP dental ceramics, Regen Biomater 2 (2015) 239–244.
[65] P.F. Cesar, A. Della Bona, S.S. Scherrer, M. Tholey, R. van Noort, A. Vichi, et al., ADM guidance—ceramics: Fracture toughness testing and method selection, Dent. Mater. 33 (2017) 1–10.
[66] K. Lundberg, L. Wu, E. Papia, The effect of grinding and/or airborne-particle abrasion on the bond strength between zirconia and veneering porcelain: a systematic review, Acta Biomater Odontol Scand 3 (2017) 8–20.
[67] D.M. Qeblawi, C.A. Muñoz, J.D. Brewer, E.A. Monaco, The effect of zirconia surface treatment on flexural strength and shear bond strength to a resin cement, J. Prosthet. Dent 103 (2010) 210–220.
[68] T. Miyazaki, T. Nakamura, H. Matsumura, S. Ban, T. Kobayashi, Current status of zirconia restoration, J Prosthodont Res 57 (2013) 236–261.
[69] M. Inokoshi, J. De Munck, S. Minakuchi, B. Van Meerbeek, Meta-analysis of bonding effectiveness to zirconia ceramics, J. Dent. Res. 93 (2014) 329–334.
[70] E. Bergamo, W. da Silva, P. Cesar, A. Del Bel Cury, Fracture load and phase transformation of monolithic zirconia crowns submitted to different aging protocols, Operat. Dent. 41 (2016) E118–E130.
[71] E.G.C. Tzanakakis, I.G. Tzoutzas, P.T. Koidis, Is there a potential for durable adhesion to zirconia restorations? A systematic review, J. Prosthet. Dent 115 (2016) 9–19.